ESR Spectra of Some Allene Radicals in Low-Temperature Matrices

Yoshihiro KUBOZONO,† Hiroki UJITA, Makoto OKADA, Masafumi ATA,†† Yoshihisa MATSUDA, and Yasuhiko GONDO*
Department of Chemistry, Faculty of Science, Kyushu University 33, Hakozaki, Higashiku, Fukuoka 812
(Received November 20, 1991)

ESR spectra of the radicals of allene (1,2-propadiene) derivatives generated by ^{60}Co γ-ray irradiation in halocarbon matrices have been observed at low temperatures. The geometrical structures of the radicals have been determined from the experimental ESR spectra and with the aid of semiempirical MO calculations invoking the UHF-AM1 and UHF-MNDO methods. After exposure of the allene derivatives to ^{60}Co γ-ray in some halocarbon matrices at 77 K, the temperature raising gave rise to neutral radicals such as allylic and/or deprotonation-type radicals; these thermal reactions have been investigated in detail.

The molecular and electronic structures as well as the reactions of alkene and alkadiene radical cations in low temperature matrices have been studied by many investigators.[1-10] Recently, Sjöqvist et al.[4] have studied the geometrical structure and thermal reactions of *trans*- and *cis*-3-hexene radical cations in halocarbon matrices with the aid of MNDO and AM1 calculations,[11-14] showing that the *trans*- and *cis*-3-hexene radical cations in CCl_3F are planar and the cation radical of *trans*-3-hexene in CCl_2FCClF_2 transforms to an allylic radical above 100 K.[4] The thermal and radiochemical reactions of alkadienes such as *cis*- and *trans*-1,3-pentadiene have been investigated by Fujisawa et al.[5] The radical cations of *cis*- and *trans*-1,3-pentadiene were found to isomerize into cyclopentene radical cations.[5] Williams et al. have reported the stereospecific formation of the chair-form cyclohexane-1,4-diyl radical cation from 1,5-hexadiene in some matrices;[6] the cyclization has also been found for 2,5-dimethyl-1,5-hexadiene in CCl_3CF_3.[7] Nevertheless, the X-ray irradiation in CCl_4 and CCl_3F frozen solutions containing 2,5-dimethyl-2,4-hexadiene did not yield such a cyclic radical, but the radical cation.[8]

The ESR investigation of allene radical was carried out for the first time by Takemura and Shida in CCl_3F, concluding that the radical cation of allene is distorted from D_{2d} to D_2 symmetry with the skew angle of 30—40°.[9]

In the present paper, the geometrical and electronic structures of various radicals of the allene derivatives, 1,2-butadiene (1,2-BD), 3-methyl-1,2-butadiene (3-M-1,2-BD), 1,2-pentadiene (1,2-PD) and 2,4-dimethyl-2,3-pentadiene (tetramethylallene; 2,4-DM-2,3-PD), have been studied on the basis of the experimental ESR spectra with the aid of semiempirical MO calculations. The radiochemical and thermal reactions of the allenes have been discussed in connection with the matrix properties.

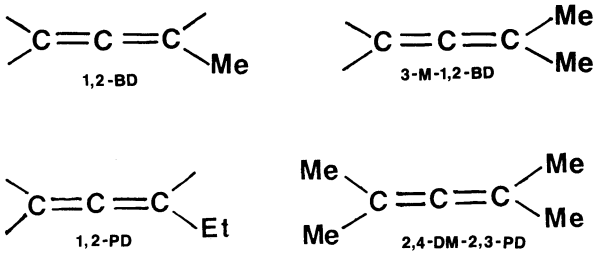

Experimental

Commercially available alkadienes, 1,2-BD, 3-M-1,2-BD, 1,2-PD (Tokyo Kasei), 2,4-DM-2,3-PD (Aldrich), and halocarbons, CCl_3F, CCl_3CF_3, CCl_2FCCl_2F, and CCl_2FCClF_2 (Tokyo Kasei) were used as received. Samples of solid solutions containing small amounts of alkadienes (ca. 0.2—4 vol%) in the various halocarbons were prepared with the standard vacuum technique. The radicals were generated by ^{60}Co γ-ray irradiation of the samples at 77 K at a total dose of 0.7 Mrad (1 Mrad=10^4 J kg^{-1}).

ESR measurements were carried out with an X-band ESR spectrometer (Echo Electronics) combined with an electromagnet (JEOL, JM-360) and/or a JEOL RE3X ESR spectrometer. The sample temperatures were carefully regulated using temperature controllers (JEOL, UTC-2AX/JES-VT-3AT and/or Oxford Instruments E900 helium flow cryostat).

Results and Discussion

General Remarks. The structures and reactions of the radicals of the allene derivatives will be discussed on the basis of the ESR data, as summarized in Table 1, and MO calculations. The theoretical UHF-INDO hyperfine coupling (hfc) constants have been calculated on the basis of the molecular geometries optimized by means of the single-point UHF-AM1 and UHF-MNDO methods,[11-14] and these theoretical hfc constants will be referred to as the hfc(A) and hfc(M) ones, respectively. The ground-state total energies optimized with the UHF-AM1 and UHF-MNDO methods will be referred to as

† Present address: Department of Chemistry, Okayama University, Tsushima, Okayama 700.

†† Present address: SONY Central Research Center, Yokohama 240.

Table 1. ESR Parameters of Allene-Derivative Radicals in Halocarbon Matrices[a)]

Radical[b)]	Matrix	T	Hfc constants/G			Line width
		K	a^{CH_3}	a^{CH_2}	a^{CH}	ΔH/G
$CH_2CC(Me)H^{+\cdot}$	CCl_3CF_3	80	24.3	33.2	8.9	4.2
$C(Me)HCHCH_2\cdot$	CCl_2FCCl_2F	133	16.5	13.9	3.8, 14.9	1.5
$CH_2CC(Me)_2^{+\cdot}$	CCl_3CF_3	138	14.2	33.8		2.4
	CCl_3F	60	14.2	33.8		4.0
	CCl_2FCClF_2	70	14.2	33.8		8.0
$CHCC(Me)_2\cdot$	CCl_2FCClF_2	100	17.9		11.5	1.9
$CH_2CC(Et)H^{+\cdot}$	CCl_3CF_3	133		25.4[c)]	9.3	4.9
	CCl_2FCCl_2F	77		25.4[c)]	9.3	7.9
$C(Me)_2CC(Me)_2^{+\cdot}$	CCl_3CF_3	70	8.3			3.3
	CCl_3F	70	8.7			2.7
	CCl_2FCCl_2F	70	8.5			4.2
	CCl_2FCClF_2	110	8.3			3.0

a) 1G=0.1 mT. b) See figure captions and text. c) These constants refer to the hfc constants of CH_2 and ethyl methylene protons.

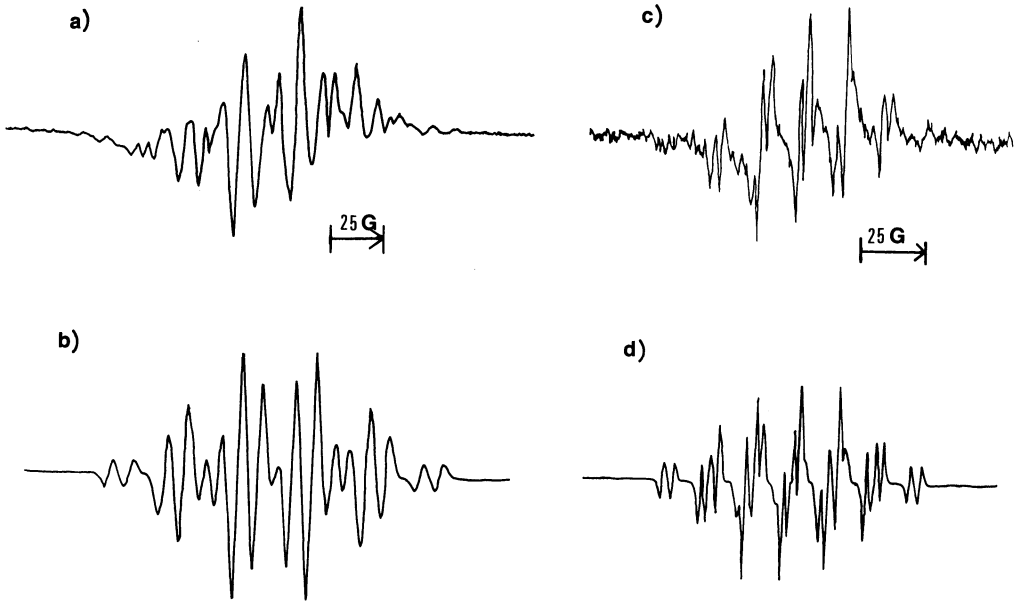

Fig. 1. ESR spectrum of 1,2-BD$^{+\cdot}$, $CH_2CC(Me)H^{+\cdot}$, in CCl_3CF_3 observed at 80 K (a) and the spectrum simulated with the ESR parameters of Table 1 (b). ESR spectrum observed at 133 K of trans-2-buten-1-yl radical generated by ^{60}Co γ-ray irradiation of 1,2-BD in CCl_2FCCl_2F (c) and the spectrum simulated in a similar manner (d).

the AM1 and MNDO energies, respectively.

Radical Species Derived from 1,2-BD. The ESR spectrum of 1,2-BD radical cation (1,2-BD$^{+\cdot}$), $CH_2CC(Me)H^{+\cdot}$, in CCl_3CF_3 observed at 80 K is shown in Fig. 1(a). The spectrum remained unchanged with increasing temperature. Figure 1(b) shows the spectrum simulated with the ESR parameters of a^{CH}(1H)= 8.9 G (1 mT=10 G), a^{CH_2}(2H)=33.2 G, a^{CH_3}(3H)=24.3 G and a Gaussian peak-to-peak width ΔH=4.2 G; the simulation reproduces the observation, as can be seen from Fig. 1(b), except for some outer lines. The equivalent hfc constants of the methyl protons indicate that the methyl group rotates freely on the time scale of ESR. Figures 2(a) and (b) show the hfc(A) and hfc(M) constants for 1,2-BD$^{+\cdot}$, respectively, as functions of the skew angle ϕ under the constraint of C_2 symmetry. The hfc(A) and hfc(M) constants of a^{CH_2} for ϕ=50—60° and 60—70°, respectively, are in good agreement with the experimental. As for a^{CH} and a^{CH_3}, the hfc(A) constants for ϕ=50—60° and hfc(M) constants for ϕ=60—70° agree approximately with the experimental. However, both of the AM1 and MNDO energies reach the minima near ϕ=45°. Thus, we conclude that 1,2-BD$^{+\cdot}$ takes a skew angle ϕ=50—60° by adopting the UHF-AM1 calculations, since the discrepancy between the best ϕ for the ESR data and that for the total energy is relatively small in the UHF-AM1 calculations. For a more strict discussion, the matrix effects should be taken into account.

The ESR spectrum observed at 77 K for the γ-

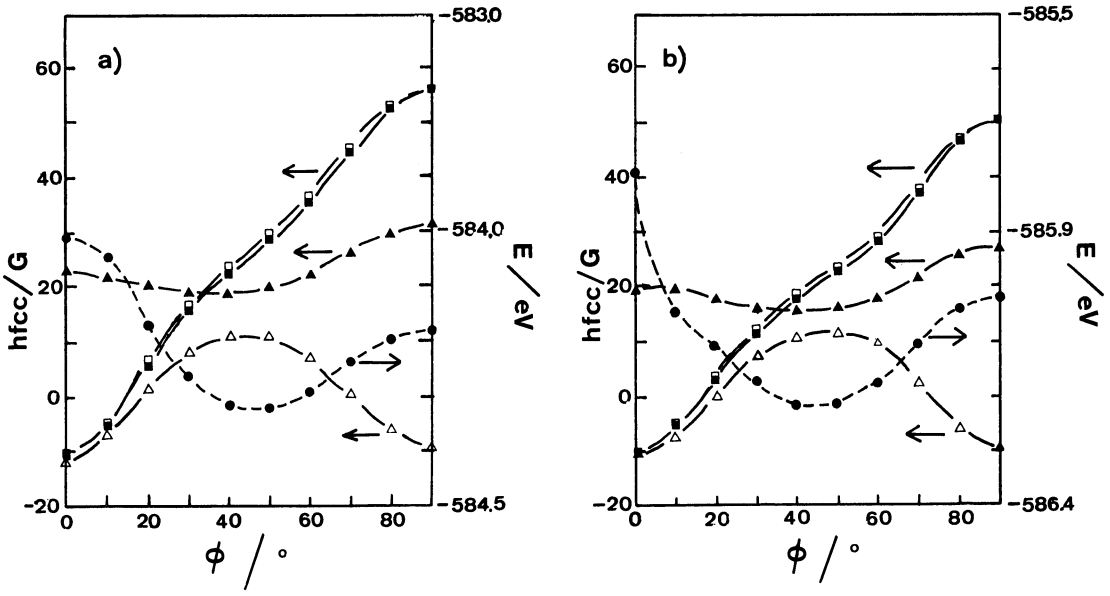

Fig. 2. The hfc(A) (a) hfc(M) (b) constants (hfcc) and the AM1 (a) and MNDO (b) energies for 1,2-BD$^{+\cdot}$. For notation, see text. □, ■: a^{CH_2}, ▲: a^{CH_3}, △: a^{CH}, ●: total energy.

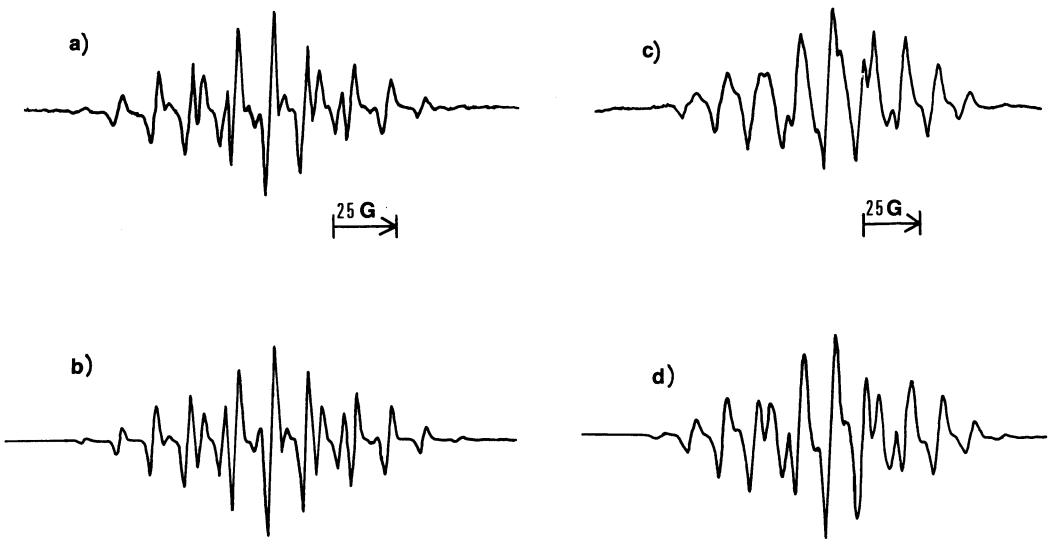

Fig. 3. ESR spectra of 3-M-1,2-BD$^{+\cdot}$, $CH_2CC(Me)_2^{+\cdot}$ observed in CCl_3CF_3 at 138 K (a) and in CCl_3F at 60 K (c). The spectra (b) and (d) simulated as in Fig. 1 refer to the observed (a) and (c), respectively.

irradiated CCl_2FCCl_2F solution of 1,2-BD cannot be ascribed to 1,2-BD$^{+\cdot}$, but to unidentified species. The ESR spectrum observed at 133 K is shown in Fig. 1(c). The spectrum simulated with $a^{CH_3}(3H)=16.5$ G, $a^{CH}(1H)=3.8$ G, $a^{CH}(1H)=14.9$ G, and $a^{CH_2}(2H)=13.9$ G is shown in Fig. 1(d). The ESR spectrum is the same as that of the CCl_2FCCl_2F solution of trans-2-butene observed at 123 K after irradiation at 77 K, as reported by Fujisawa et al.[10] Consequently, the species observed at 133 K can be attributed to the *trans*-2-buten-1-yl radical, $C(Me)HCHCH_2\cdot$. The allylic radical was also observed at 80 K for the CCl_2FCClF_2 solution of 1,2-BD after irradiation at 77 K. The temperature for formation of the allylic radical depends on the matrices. It is noteworthy that 1,2-BD gives rise exclusively to the trans-2-buten-1-yl radical.

Radical Species Derived from 3-M-1,2-BD. The ESR spectrum of 3-M-1,2-BD$^{+\cdot}$, $CH_2CC(Me)_2^{+\cdot}$, in CCl_3CF_3 observed at 138 K is shown in Fig. 3(a). The spectrum simulated with $a^{CH_3}(6H)=14.2$ G, $a^{CH_2}(2H)=33.8$ G and $\Delta H=2.4$ G is given in Fig. 3(b). The methyl group rotates freely as in 1,2-BD$^{+\cdot}$. The a^{CH_3} of 3-M-1,2-BD$^{+\cdot}$ is smaller than that of 1,2-BD$^{+\cdot}$. Nevertheless, the summation of $a^{CH_3}(6H)$ for 3-M-1,2-BD$^{+\cdot}$ (14.2 G×6) is

almost equal to that of a^{CH_3}(3H) and a^{CH}(1H) for 1,2-BD$^{+\cdot}$ (24.3 G×3+8.9 G). The a^{CH_2} for 3-M-1,2-BD$^{+\cdot}$ (33.8 G) is equal to that for 1,2-BD$^{+\cdot}$ (33.2 G). Figures 4(a) and (b) show the hfc(A) and hfc(M) constants, respectively; the a^{CH_2} changes markedly when ϕ is varied from 0° to 90°, and the total-energy curves exhibit minima near ϕ=45°. The ϕ was determined to be 40—50° by comparing the experimental a^{CH_2}(2H) with the theoretical. The hfc(M) constant of a^{CH_2}(2H) fits well the experimental at ϕ=50—60°, but the ϕ value deviates by ca. 10° from that for the total-energy minimum. On the other hand, the range of ϕ=40—50° estimated by the hfc(A) constants agrees with that for the total-energy minimum.

The ESR spectra of 3-M-1,2-BD$^{+\cdot}$ were observed at 30—135 K after γ-ray irradiation of 3-M-1,2-BD in CCl_3F at 77 K; Fig. 3(c) shows the ESR spectrum observed at 60 K which can be simulated with the same hfc constants as those in CCl_3CF_3 but with a broader width of ΔH=4.0 G, as is shown in Fig. 3(d). The spectral resolution is better in CCl_3CF_3 than in CCl_3F.

The ESR spectrum observed at 70 K after ^{60}Co γ-ray

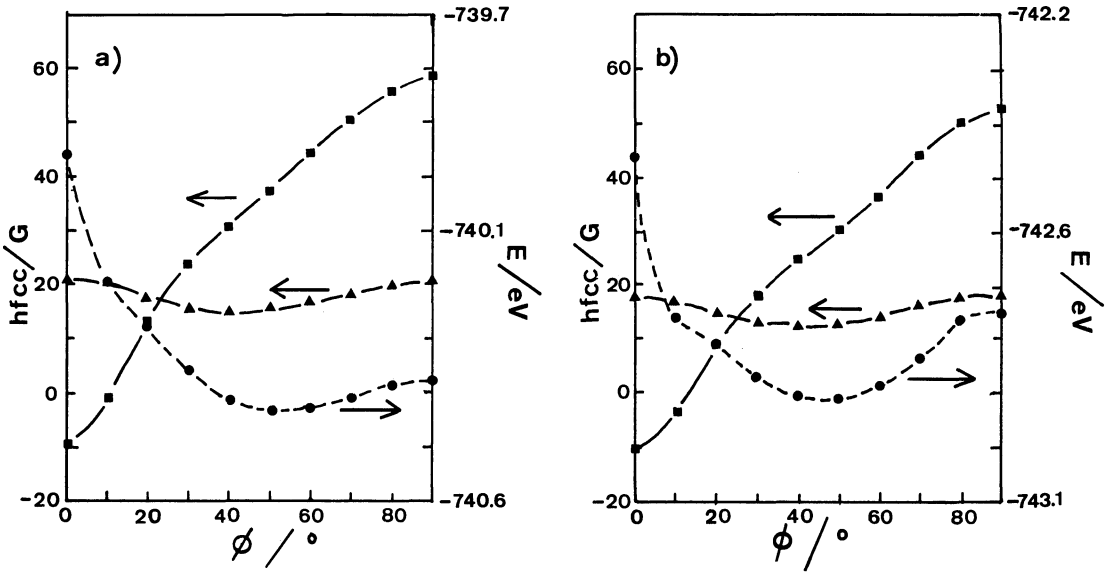

Fig. 4. The hfc(A) (a) and hfc(M) (b) constants (hfcc) and the AM1 (a) and MNDO (b) energies for 3-M-1,2-BD$^{+\cdot}$. For notation, see text. ■: a^{CH_2}, ▲: a^{CH_3}, ●: total energy.

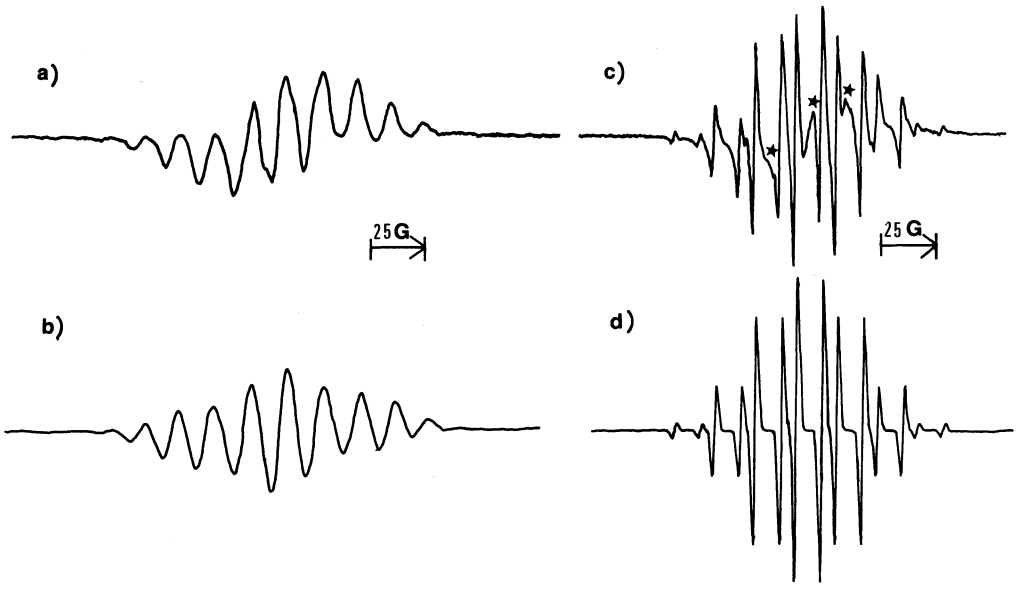

Fig. 5. ESR spectra, observed at 70 K (a) and 100 K (c), of the radicals generated by exposure of 3-M-1,2-BD to ^{60}Co γ-rays in CCl_2FCClF_2 at 77 K. The respective spectra are assigned to 3-M-1,2-BD$^{+\cdot}$ and the deprotonation-type 3-methyl-1,2-butadien-1-yl radical, $CHCC(Me)_2\cdot$. The spectra (b) and (d) simulated as in Fig. 1 refer to the observed (a) and (c), respectively.

irradiation of the CCl_2FCClF_2 solution of 3-M-1,2-BD at 77 K is composed of thirteen lines, as is shown in Fig. 5(a). The species disappeared and another radical appeared with increasing temperature. The species obtained at 70 K can be attributed to 3-M-1,2-$BD^{+\cdot}$. The ESR spectrum can be simulated with the same hfc constants as those observed for 3-M-1,2-$BD^{+\cdot}$ in CCl_3CF_3 at 138 K and with a broader Gaussian line width, ΔH=8.0 G, as is shown in Fig. 5(b). The ESR spectrum observed at 100 K shown in Fig. 5(c), is composed of doublet septet lines, with the total splitting of ca. 120 G. The total splitting is smaller than those of 3-M-1,2-$BD^{+\cdot}$ in CCl_3CF_3 and CCl_3F which are ca. 150 G. The spectrum simulated with a^{CH}(1H)=11.5 G, a^{CH_3}(6H)= 17.9 G, and ΔH=1.9 G is given in Fig. 5(d). The species observed at 100 K can be attributed to the deprotonation-type neutral 3-methyl-1,2-butadien-1-yl radical, $CHCC(Me)_2$·. Thus, the 3-M-1,2-$BD^{+\cdot}$ has been found to undergo thermal deprotonation. The lines marked with stars in the ESR spectrum at 100 K are attributed to the remaining 3-M-1,2-$BD^{+\cdot}$; the 3-M-1,2-$BD^{+\cdot}$ did not completely disappear even at 100 K. The occurrence of the thermal reaction, an ion-molecule reaction, reflects the softness of the CCl_2FCClF_2 matrix.

Figures 6(a) and (b) show the hfc(A) constants of a^{CH}(1H) and a^{CH_3}(6H) and the corresponding hfc(M) constants, respectively, which were evaluated under the constraint of C_2 symmetry. These theoretical hfc constants agree with the experimental qualitatively; the theoretical a^{CH_3}(6H) values are overestimated as compared with the experimental, whereas the absolute value of the thoretical a^{CH}(1H) value, which is negative due to the spin exchange interaction, is underestimated. The geometry optimized by the UHF-MNDO method reproduces the experimental hfc constants more consistently than that by the UHF-AM1.

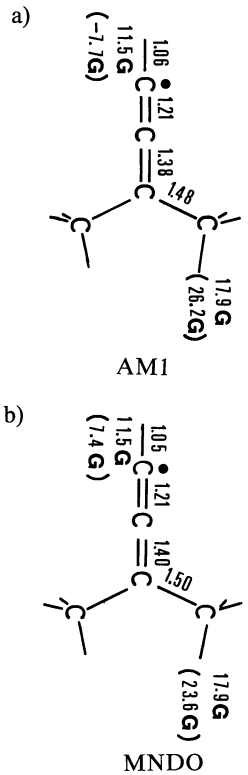

Fig. 6. Geometries calculated with the UHF-AM1 (a) and MNDO (b) methods, together with the experimental hfc constants as well as the hfc(A) (a) and hfc(M) (b) (in parentheses) for the deprotonation-type 3-methyl-1,2-butadien-1-yl radical. The bond lengths are given in Å. For notation, see text.

The temperature dependence of the ESR spectrum of the irradiated 3-M-1,2-BD in CCl_2FCCl_2F matrix is similar to that in CCl_2FCClF_2; the 3-M-1,2-$BD^{+\cdot}$ was observed at 77 K, and it is converted gradually into the deprotonation-type neutral 3-methyl-1,2-butadien-1-yl radical, with increasing temperature. The reactions of 3-M-1,2-BD in CCl_3CF_3 and CCl_3F are different from those in CCl_2FCCl_2F and CCl_2FCClF_2. This reflects the difference in matrix rigidity; the slow diffusion of the cation radical in a softened matrix above 77 K induces the deprotonation.

Radical Species Derived from 1,2-PD. Figure 7(a) shows the ESR spectrum of 1,2-$PD^{+\cdot}$, $CH_2CC(Et)H^{+\cdot}$, in CCl_3CF_3 observed at 133 K, exhibiting the quintet doublet lines. Figure 7(b) shows the spectrum simulated with the hfc constant of 25.4 G due to the four equivalent protons and 9.3 G due to the remaining proton, and the line width ΔH=4.9 G. The four equivalent protons can be assigned to the two CH_2 protons and two methylene protons in the ethyl group, while the other proton, to a CH proton. The theoretical hfc constants and total energies evaluated in the above-mentioned manner are shown in Fig. 8; the experimental a^{CH_2}(2H) of 25.4 G due to CH_2 protons and a^{CH}(1H) of

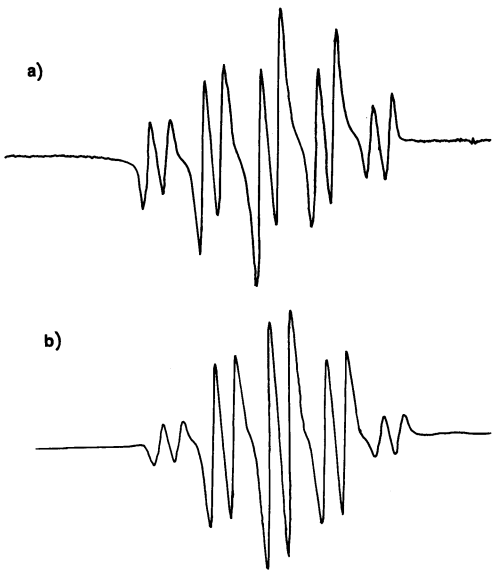

Fig. 7. ESR spectrum of 1,2-$PD^{+\cdot}$, $CH_2CC(Et)H^{+\cdot}$, in CCl_3CF_3 observed at 133 K (a) and the spectrum simulated (b) as in Fig. 1.

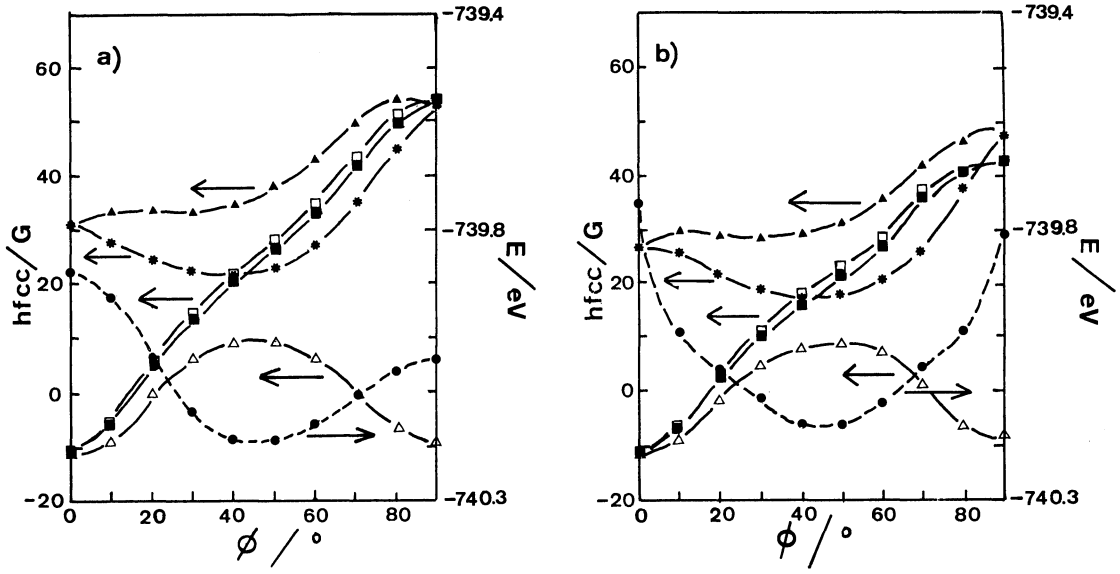

Fig. 8. The hfc(A) (a) and hfc(M) (b) constants (hfcc) and the AM1 (a) and MNDO (b) energies for 1,2-PD$^{+\cdot}$. For notation, see text. □, ■: a^{CH_2} for CH_2 protons, ▲, ●: a^{CH_2} for ethyl methylene protons, △: a^{CH}, ●: total energy.

9.3 G are reproduced for ϕ=40—50° in the hfc(A) calculation, and for ϕ=50—60° in the hfc(M), as is seen from Figs. 8(a) and 8(b), respectively. On the other hand, the theoretical hfc constants due to methylene protons in the ethyl group deviate slightly from the experimental one, 25.4 G; the hfc constant due to one methylene proton is overestimated, while that due to the other is underestimated. The mean value of these two theoretical hfc constants agrees approximately with the experimental one, for ϕ=40—50° in the hfc(A) calculation, and for ϕ=50—60° in the hfc(M). These results indicate that the hfc constants due to the methylene protons in the ethyl group of 1,2-PD$^{+\cdot}$ in CCl_3CF_3 are dynamically averaged at 133 K. The dynamical averaging of the hfc constants due to methylene protons requires the rapid site exchange of the two protons. The AM1 and MNDO energy curves give the minima near ϕ=ca. 45°. Thus, we conclude that 1,2-PD$^{+\cdot}$ in CCl_3CF_3 takes ϕ=40—50° in adopting the hfc(A) constants, since the ϕ=40—50° determined for the hfc(A) constants is consistent with the ϕ=ca. 45° for the total energy minimum. The experimental results can be reproduced consistently, with the geometry of ϕ=40—50° subject to the rapid site exchange ($<10^{-9}$ s) of the methylene protons.

The ESR spectrum of 1,2-PD$^{+\cdot}$ was observed at 77 K after exposing 1,2-PD in CCl_2FCCl_2F to ^{60}Co γ-ray at 77 K. It was converted into another species at 110 K, and the observed ESR spectrum was somewhat complicated. The species involved have not yet been identified.

Radical Species Derived from 2,4-DM-2,3-PD. Figure 9(a) shows the ESR spectrum of 2,4-DM-2,3-PD$^{+\cdot}$, $C(Me)_2CC(Me)_2^{+\cdot}$, in CCl_3F observed at 70 K,

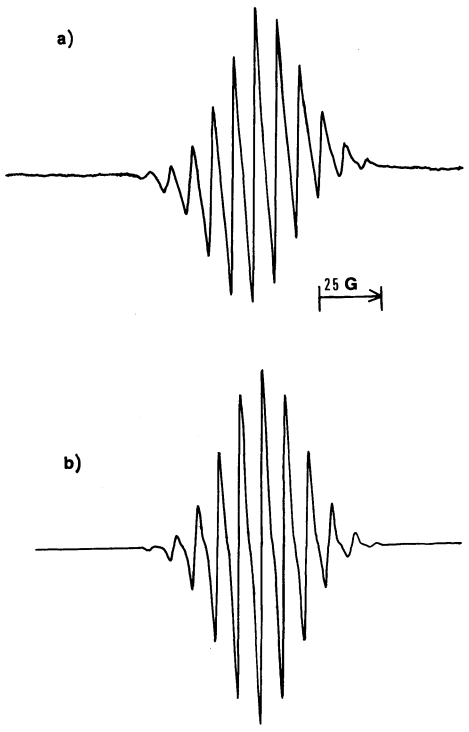

Fig. 9. ESR spectrum of 2,4-DM-2,3-PD$^{+\cdot}$, $C(Me)_2$-$CC(Me)_2^{+\cdot}$ in CCl_3F observed at 70 K (a) and the spectrum simulated (b) as in Fig. 1.

which is isotropic and composed of thirteen lines, indicating the free rotation of the methyl groups at 70 K on the time scale of ESR. Figure 9(b) shows the spectrum simulated with the hfc constant of 8.7 G for the twelve methyl protons and ΔH=2.7 G. The 2,4-DM-2,3-PD$^{+\cdot}$ was also observed in CCl_3CF_3, CCl_2FCClF_2 and

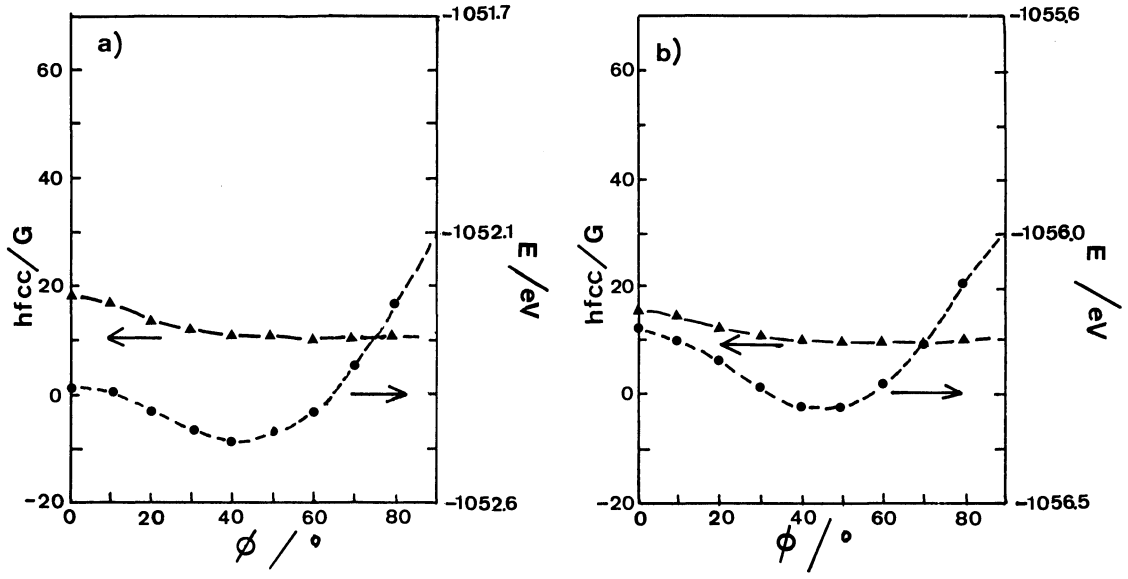

Fig. 10. The hfc(A) (a) and hfc(M) (b) constants (hfcc) and the AM1 (a) and MNDO (b) energies for 2,4-DM-2,3-PD$^{+\cdot}$. For notation, see text. ▲: a^{CH_3}, ●: total energy.

CCl_2FCCl_2F at 70—90 K after ^{60}Co γ-ray irradiation at 77 K, exhibiting the isotropic thirteen lines. These spectra were the same as that in CCl_3F. In the course of the present study, Qin and Trifunac reported the ESR spectra of 2,4-DM-2,3-PD$^{+\cdot}$ in CCl_3F, CCl_2FCClF_2, and CCl_4 matrices,[15] which are the same as those reported in the present paper. The matrix dependence of the hfc constant due to methyl protons is not appreciable for 2,4-DM-2,3-PD$^{+\cdot}$.

Figures 10(a) and (b) show the hfc(A) and hfc(M) constants for the methyl protons and the AM1 and MNDO energies evaluated under the constraint of D_2 symmetry. The hfc(A) and hfc(M) constants for ϕ=40—80° are in good agreement with the experimental one; the AM1 and MNDO energy curves give the minima at ϕ=ca. 40° and ϕ=40—50°, respectively. We conclude that the 2,4-DM-2,3-PD$^{+\cdot}$ takes ϕ=40—50°, judging from the total energy curve. The geometry of 2,4-DM-2,3-PD$^{+\cdot}$, however, cannot definitely be determined owing to the small variation of the hfc constant of the methyl protons as a function of the skew angle.

The ESR spectrum of 2,4-DM-2,3-PD$^{+\cdot}$ in CCl_2FCCl_2F observed at 70 K changed to another pattern at 110 K, as can be seen from Figs. 11(a) and (b). The spectrum observed at 110 K is composed of thirteen lines ascribed to 2,4-DM-2,3-PD$^{+\cdot}$ and the other lines to another species. The ESR spectrum of 2,4-DM-2,3-PD$^{+\cdot}$ changed with increasing temperature in CCl_3CF_3 above 140 K, while the ESR spectra of 2,4-DM-2,3-PD$^{+\cdot}$ in CCl_3F and CCl_2FCClF_2 remained unchanged.

Remarks on the Electronic Structure. In the alkyl-substituted allene radical cations, both hyperconjugation and changes in molecular geometry are the important factors determining the electronic structure. As can be seen from Table 1, the methyl proton and ethyl methylene

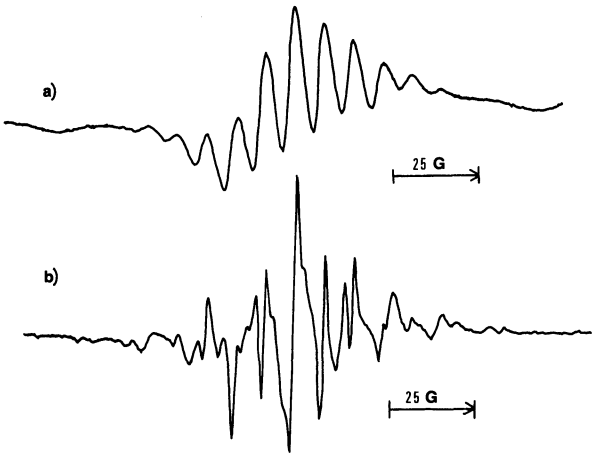

Fig. 11. ESR spectra, observed at 70 K (a) and 110 K (b), of the radicals generated by exposure of 2,4-DM-2,3-PD to ^{60}Co γ-rays in CCl_2FCCl_2F at 77 K. The spectrum (a) is ascribed to 2,4-DM-2,3-PD$^{+\cdot}$, while the spectrum (b), to the remaining 2,4-DM-2,3-PD$^{+\cdot}$ and other species.

proton hfc constants decrease monotonically with increasing number of alkyl groups. However, the CH_2 proton hfc constants in 1,2-BD$^{+\cdot}$, 3-M-1,2-BD$^{+\cdot}$, and 1,2-PD$^{+\cdot}$ have no definite relation with this decrease tendency. In particular, the effect of the CH_3 group in the ethyl group of 1,2-PD$^{+\cdot}$ on the CH_2 proton hfc constant is seemingly very interesting, since the CH_2 proton hfc constant of 1,2-PD$^{+\cdot}$ is quite different from that of 1,2-BD$^{+\cdot}$, whereas the other proton hfc constants of these two radical cations are similar to each other. Thus, the electronic structure of the alkyl-substituted allene radical cations is an interesting subject to be studied by means of more advanced approaches than adopted in the present work.

Conclusion

From the hfc(A) and hfc(M) constants, the skew angle is estimated to fall in the ranges ϕ=40—50° and 50—60°, respectively, for all allene radical cations studied. On the other hand, the AM1 and MNDO total-energy curves give minima near ϕ=45° for all radical cations studied, in contrast to neutral molcules; the geometries of 1,2-BD, 3-M-1,2-BD, 1,2-PD, and 2,4-DM-2,3-PD are determined to give ϕ=90° either with the UHF-MNDO or with the UHF-AM1 method. The geometries of allene radical cations were slightly affected by the variation of the alkyl substituents. The geometries determined in the present study seem to be reasonable in view of the total energies.

The mechanism of the dynamical averaging of the methylene-proton hfc constants in 1,2-$PD^{+\cdot}$ is left to be studied in detail. The thermally-generated unidentified radicals should be investigated further, for which resonance Raman spectroscopic studies are also in progress.

The authors wish to thank Professors T. Matsuo and H. Nakamura of Kyushu University for allowing us to use an ESR spectrometer (JEOL, RE3X) equipped with a liquid helium flow cryostat. We are grateful to Professor M. Shiotani of Hiroshima University for his valuable suggestions and Mr. M. Aoyagi for his assistance. The MOPAC Ver. 5.0 was used for UHF-AM1 and UHF-MNDO calculations. All MO calculations were carried out on a FACOM M-780/20 computer at the Computer Center of Kyushu University.

References

1) T. Ichikawa and P. K. Ludwig, *J. Am. Chem. Soc.*, **91**, 1023 (1969).
2) T. Shida, Y. Egawa, H. Kubodera, and T. Kato, *J. Chem. Phys.*, **73**, 5963 (1980).
3) K. Toriyama, K. Nunome, and M. Iwasaki, *Chem. Phys. Lett.*, **107**, 86 (1984).
4) L. Sjöqvist, M. Shiotani, and A. Lund, *Chem. Phys.*, **141**, 417 (1990).
5) J. Fujisawa, T. Takayanagi, S. Sato, and K. Shimokoshi, *Bull. Chem. Soc. Jpn.*, **61**, 1527 (1988).
6) F. Williams, Q.-X. Guo, D. C. Bebout, and B. K. Carpenter, *J. Am. Chem. Soc.*, **111**, 4133 (1989).
7) Y. Kubozono, M. Aoyagi, H. Nakamura, Y. Matsuda, M. Ata, and Y. Gondo, *Chem. Phys. Lett.*, to be published.
8) L. S. Prasad, R. S. Ding, H.-Q. Wang, E. G. Bradford, and L. D. Kispert, *Chem. Phys. Lett.*, **151**, 443 (1988).
9) Y. Takemura and T. Shida, *J. Chem. Phys.*, **73**, 4133 (1980).
10) J. Fujisawa, S. Sato, K. Shimokoshi, and T. Shida, *J. Phys. Chem.*, **89**, 5481 (1985).
11) M. J. S. Dewar and W. Thiel, *J. Am. Chem. Soc.*, **99**, 4899 (1977).
12) M. J. S. Dewar, E. G. Zoebisch, E. F. Healy, and J. J. P. Stewart, *J. Am. Chem. Soc.*, **107**, 3902 (1985).
13) J. J. P. Stewart, *QCPE Bull.*, **9**, 10 (1989).
14) T. Hirano, *JCPE Newsletter*, **1**, 10 (1989).
15) X.-Z. Qin and A. D. Trifunac, *J. Phys. Chem.*, **95**, 6466 (1991).